Available online at www.sciencedirect.com

ScienceDirect

Ceramics International 40 (2014) 4575–4578

CERAMICS INTERNATIONAL

www.elsevier.com/locate/ceramint

Influence of precursor Bi^{3+}/Fe^{3+} ion concentration on hydrothermal synthesis of $BiFeO_3$ crystallites

L.J. Di[b], H. Yang[a,b,*], T. Xian[a,b], R.S. Li[b], Y.C. Feng[b], W.J. Feng[a]

[a]State Key Laboratory of Gansu Advanced Non-ferrous Metal Materials, Lanzhou University of Technology, Lanzhou 730050, People's Republic of China
[b]School of Science, Lanzhou University of Technology, Lanzhou 730050, People's Republic of China

Received 8 July 2013; received in revised form 29 August 2013; accepted 29 August 2013
Available online 7 September 2013

Abstract

In this study we investigated the effect of precursor Bi^{3+}/Fe^{3+} ion concentration on the hydrothermal synthesis of $BiFeO_3$ crystallites. It is demonstrated that the phase-purity and morphology of the products is highly dependent on the metal ion concentration. Phase-pure $BiFeO_3$ crystals can be prepared at the Bi^{3+}/Fe^{3+} ion concentration ranging from 0.025 to 0.0625 M. The samples prepared at $n(Bi^{3+}/Fe^{3+})=0.025$, 0.0375, 0.05, and 0.0625 M, are composed, respectively, of cuboid-like particles (100–200 nm), regular spherical agglomerates (30–40 μm) made up of irregular grains with size about several hundred nanometers, irregular flower-like clusters formed from irregular grains of several hundred nanometers in size, and octahedron-shaped particles (500–600 nm). These samples have a similar bandgap energy of 2.20 eV and exhibit a typical antiferromagnetic behavior at room temperature.

Keywords: $BiFeO_3$; Crystallites; Hydrothermal method; Bi^{3+}/Fe^{3+} concentration

1. Introduction

Bismuth ferrite ($BiFeO_3$) with a rhombohedrally distorted perovskite structure is one of the best-known multiferroic materials. Due to the coexistence of ferroelectric and antiferromagnetic orders up to quite high temperatures as well as magnetoelectric coupling between them [1–3], $BiFeO_3$ is regarded to be a highly promising multiferroic system for potential applications. Furthermore, $BiFeO_3$ is an interesting semiconductor with bandgap energy of about 2.0 eV, which exhibits a pronounced photocatalytic activity toward the degradation of various organic dyes under visible-light irradiation [4–8]. The overall properties of a material depend on numerous factors like its structure, defect, dimension, size, and morphology. For example, nanosized $BiFeO_3$ tends to exhibit enhanced photocatalytic activity and also present weak ferromagnetism that is absent in its bulk form [7–13]. To tailor and/or enhance its properties, various techniques have been widely used to prepare $BiFeO_3$ nano/micro crystals [4–18]. Among them, the hydrothermal route offers an advantage in controlling the product morphology. The main operating parameters that have been extensively investigated include mineralizer concentration, organic additive, reaction temperature, and reaction time [5,6,11–15]. However, there has been little attention paid to the effect of Bi^{3+}/Fe^{3+} ion concentration in precursor solution on the hydrothermal synthesis of $BiFeO_3$ crystallites. Here we undertake an investigation aimed at studying its effect on the phase-purity and morphology of prepared samples via a hydrothermal route.

2. Experimental

All raw materials and reagents used are of analytical grade without further purification. Equimolar amounts of $Bi(NO_3)_3 \cdot 5H_2O$ and $Fe(NO_3)_3 \cdot 9H_2O$ were dissolved in 20 mL of dilute nitric acid solution. To the mixture solution was then added 60 mL KOH solution with a concentration of 4 mol L^{-1} (M) drop by drop under magnetic stirring, and immediately a dark brown

*Corresponding author at: State Key Laboratory of Gansu Advanced Non-ferrous Metal Materials, Lanzhou University of Technology, Lanzhou 730050, People's Republic of China. Tel.: +86 931 2973783; fax: +86 931 2976040.
E-mail address: hyang@lut.cn (H. Yang).

0272-8842/$ - see front matter © 2013 Elsevier Ltd and Techna Group S.r.l. All rights reserved.
http://dx.doi.org/10.1016/j.ceramint.2013.08.134

suspension solution was formed. The suspension was ultrasonically treated for 8 min and subsequently stirred vigorously with a magnetic stirrer for 30 min to create a highly uniform mixture. The resulted mixture was sealed in a Teflon-lined stainless steel autoclave of 100 mL capacity and submitted to hydrothermal treatment at 200 °C. After 6 h of reaction, the autoclave was cooled naturally to room temperature. The resulting brown precipitate was collected and washed several times with distilled water and absolute ethanol, and then dried in a thermostat drying oven at 80 °C for 12 h to obtain final $BiFeO_3$ product. By varying the concentration of $Bi(NO)_3 \cdot 5H_2O$ and $Fe(NO)_3 \cdot 9H_2O$ from 0.0125 to 0.075 M (final concentration in autoclave), we prepared a series of $BiFeO_3$ samples.

The phase purity of the products was checked by means of X-ray powder diffraction (XRD) with Cu Kα radiation. The particle morphology was investigated by a field-emission scanning electron microscope (SEM). The ultraviolet (UV)-visible diffuse reflectance spectra were measured using a UV–visible spectrophotometer with an integrating sphere attachment. A vibrating sample magnetometer (VSM) was used to measure the magnetic hysteresis loops at room temperature.

3. Results and discussion

Fig. 1 shows the XRD patterns of $BiFeO_3$ samples prepared at different Bi^{3+}/Fe^{3+} ion concentrations in precursor solution. Phase-pure $BiFeO_3$ samples with a rhombohedral *R*3*m* structure (PDF card no. 74-2016) are seen to be formed at the metal ion concentrations ranging from 0.025 to 0.0625 M. However, when the metal ion concentration is raised up to 0.075 M or reduced down to 0.0125 M, the prepared samples present a second $Bi_2Fe_4O_9$ phase. The XRD results suggest that appropriate Bi^{3+}/Fe^{3+} ion concentrations in precursor solution are necessary in producing phase-pure $BiFeO_3$ crystals via the present hydrothermal synthesis route.

Fig. 2 shows the SEM images of the as-prepared pure $BiFeO_3$ samples, revealing that the morphology of $BiFeO_3$ crystals is highly dependent on the precursor Bi^{3+}/Fe^{3+} ion concentration. The sample prepared at $n(Bi^{3+}/Fe^{3+})=0.025$ M is mainly composed of cuboid-like particles in the size range of 100–200 nm

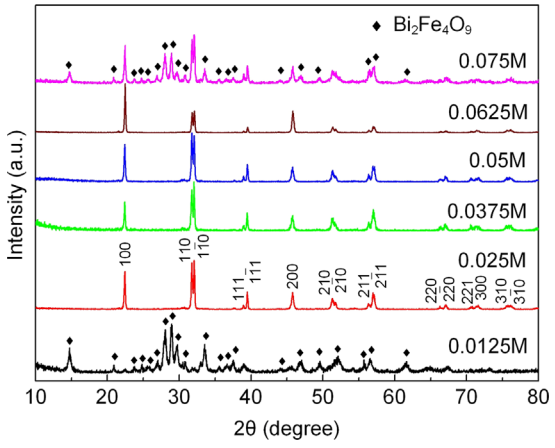

Fig. 1. XRD patterns of $BiFeO_3$ samples prepared at different Bi^{3+}/Fe^{3+} ion concentrations in precursor solution ranging from 0.0125 to 0.075 M.

(Fig. 2(a)). When $n(Bi^{3+}/Fe^{3+})=0.0375$ M, the resulted sample presents regular spherical agglomerates of 30–40 μm in diameter (Fig. 2(b)). The higher-magnification image inserted in Fig. 2(b) reveals that the spherical agglomerates are made up of irregular grains with a size of several hundred nanometers. From Fig. 2(c), one can see that the sample prepared at $n(Bi^{3+}/Fe^{3+})=0.05$ M consists of irregular flower-like clusters formed from irregular grains of several hundred nanometers in size. The SEM image shown in Fig. 2(d) reveals the synthesis of octahedron-shaped particles with size ranging from 500 to 600 nm when $n(Bi^{3+}/Fe^{3+})=0.0625$ M.

The crystallization process of $BiFeO_3$ can be simply described as follows. First, the starting materials, $Bi(NO_3)_3 \cdot 5H_2O$ and $Fe(NO_3)_3 \cdot 9H_2O$, were dissolved in dilute nitric acid to form a uniform Bi^{3+}/Fe^{3+} ion solution. Then, KOH was added to the solution, which reacted with Bi^{3+} and Fe^{3+} ions to produce amorphous $Bi(OH)_3$ and $Fe(OH)_3$ precipitates (Eqs. (1) and (2)). Finally, $Bi(OH)_3$ and $Fe(OH)_3$ reacted under the hydrothermal condition to yield $BiFeO_3$ particles (Eq. (3)). The hydrothermal formation of $BiFeO_3$ particles can be explained by the "dissolution–crystallization" mechanism [19]. According to this mechanism, the reactants underwent an attack of the mineralizer, KOH, to dissolve and form ion groups. Then $BiFeO_3$ particles were formed by nucleation, precipitation, dehydration and growth, in which the crystal growth only occurred in the region of supersaturated fluid. When varying the Bi^{3+}/Fe^{3+} ion concentration in precursor solution, the nucleation and growth process of $BiFeO_3$ particles could be changed, consequently resulting in morphologically different products. However, when the metal ion concentration was too high or too low, the requirement of supersaturation and stoichiometry for the crystallization of $BiFeO_3$ particles could be locally destroyed. Another possible reaction as indicated in Eq. (4) could take place, leading to the formation of the second $Bi_2Fe_4O_9$ phase in final product.

$$Bi^{3+} + 3OH^- \rightarrow Bi(OH)_3 \quad (1)$$

$$Fe^{3+} + 3OH^- \rightarrow Fe(OH)_3 \quad (2)$$

$$Bi(OH)_3 + Fe(OH)_3 \rightarrow BiFeO_3 + 3H_2O \quad (3)$$

$$2Bi(OH)_3 + 4Fe(OH)_3 \rightarrow Bi_2Fe_4O_9 + 9H_2O \quad (4)$$

Fig. 3(a) shows the UV–visible diffuse reflectance spectra of $BiFeO_3$ samples. In order to highlight the optical absorption features, the corresponding differential spectra are derived and shown in Fig. 3(b), where the peak wavelengths are characterized to be the absorption edges of the samples. It is seen that these samples have similar absorption peaks. According to the theoretical results [20], the absorption edge at 564 nm is attributed to the electron transition from valence band to conduction band, from which the bandgap energy (E_g) of the $BiFeO_3$ crystallites is obtained to be 2.20 eV.

Fig. 4 show the magnetic hysteresis loops of $BiFeO_3$ samples measured at room temperature. The magnetization for all samples is seen to change nearly linearly with applied magnetic field, implying a typical antiferromagnetic behavior.

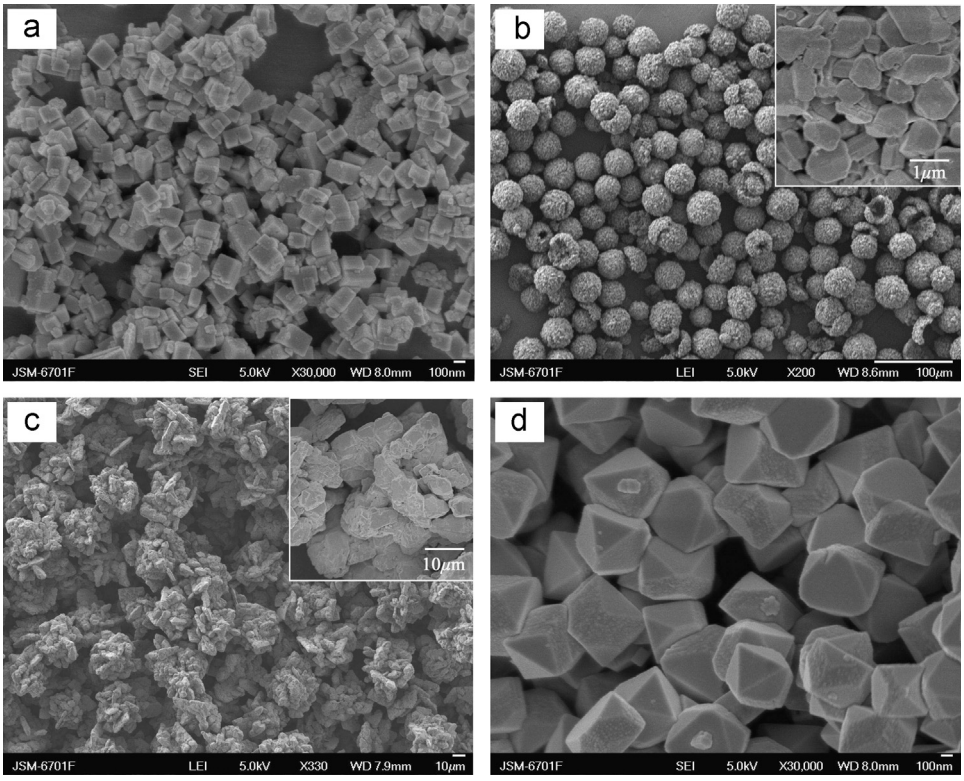

Fig. 2. SEM images of $BiFeO_3$ samples prepared at different Bi^{3+}/Fe^{3+} ion concentrations in precursor solution. (a) 0.025 M, (b) 0.0375 M, (c) 0.05 M, and (d) 0.0625 M.

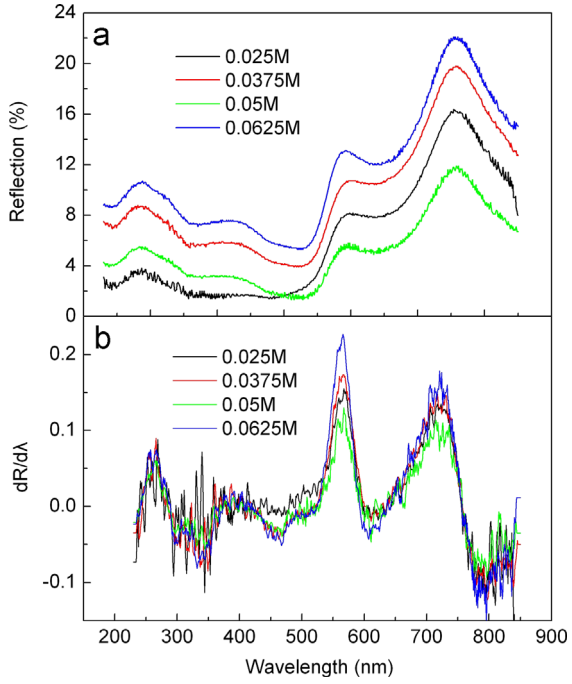

Fig. 3. (a) UV–visible diffuse reflectance spectra of $BiFeO_3$ samples and (b) the corresponding first derivative of the diffuse reflectance spectra.

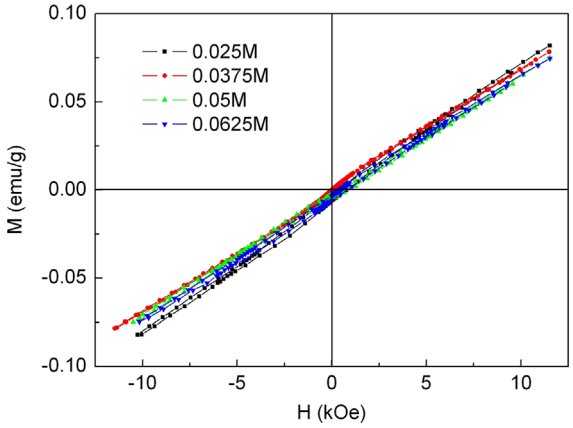

Fig. 4. Magnetic hysteresis loops of $BiFeO_3$ samples measured at room temperature.

It should be noted that weak ferromagnetism is generally observed for nanosized $BiFeO_3$ and exhibits an increasing trend with reducing the grain size [10]. This is because that the long-range helical antiferromagnetic order of $BiFeO_3$ (with a period of ~62 nm [21]) is destroyed at nanoscale, making the spin compensation incomplete. The absence of macroscopic magnetization for our $BiFeO_3$ samples indicates that they crystallize in relatively large-sized microcrystals.

4. Conclusions

A hydrothermal route was used to synthesize $BiFeO_3$ crystallites, where the effect of Bi^{3+}/Fe^{3+} ion concentration in precursor solution on the phase-purity and morphology of

the products was investigated. XRD analysis indicates that phase-pure $BiFeO_3$ crystals can be prepared at a Bi^{3+}/Fe^{3+} ion concentration of 0.025–0.0625 M. SEM observation demonstrates that the samples prepared at $n(Bi^{3+}/Fe^{3+})=$ 0.025 and 0.0625 M present cuboid-like particles (100–200 nm) and octahedron-shaped particles (500–600 nm), respectively. When $n(Bi^{3+}/Fe^{3+})=0.0375$ and 0.05 M, the resulted samples are composed, respectively, of regular spherical agglomerates (30–40 μm) and irregular flower-like clusters, both of which are made up of irregular grains with size about several hundred nanometers. UV–visible diffuse reflectance spectra show that these samples have a similar bandgap energy of 2.20 eV. Magnetic hysteresis loop measurement reveals a typical antiferromagnetic behavior for these samples at room temperature.

Acknowledgments

This work was supported by theNational Natural Science Foundation of China (Grant nos. 51262018, 50962009 and 11264023) and the Hongliu Outstanding Talents Foundation of Lanzhou University of Technology (Grant no. J201205).

References

[1] C. Tabares-Munoz, J.P. Rivera, A. Monnier, H. Schmid, Measurement of the quadratic magnetoelectric effect on single crystalline $BiFeO_3$, Japanese Journal of Applied Physics 24 (1985) 1051–1053.

[2] P. Fischer, M. Polomska, I. Sosnowska, M. Szymanski, Temperature dependence of the crystal and magnetic structures of BiFeO3, Journal of Physics C 13 (1980) 1931–1940.

[3] J. Wang, J.B. Neaton, H. Zheng, V. Nagarajan, S.B. Ogale, B. Liu, D. Viehland, V. Vaithyanathan, D.G. Schlom, U.V. Waghmare, N.A. Spaldin, K.M. Rabe, M. Wuttig, R. Ramesh, Science 299 (2003) 1719–1722.

[4] T. Soltani, M.H. Entezari, Solar photocatalytic degradation of RB5 by ferrite bismuth nanoparticles synthesized via ultrasound, Ultrasonics Sonochemistry 20 (2013) 1245–1253.

[5] J. Wei, H.Y. Li, S.C. Mao, C. Zhang, Z. Xu, B. Dkhil, Effect of particle morphology on the photocatalytic activity of BiFeO3 microcrystallites, Journal of Materials Science: Materials in Electronics 23 (2012) 1869–1874.

[6] S. Li, Y.H. Lin, B.P. Zhang, Y. Wang, C.W. Nan, Controlled fabrication of $BiFeO_3$ uniform microcrystals and their magnetic and photocatalytic behaviors, Journal of Physical Chemistry C. 114 (2010) 2903–2908.

[7] T. Xian, H. Yang, J.F. Dai, Z.Q. Wei, J.Y. Ma, W.J. Feng, Photocatalytic properties of $BiFeO_3$ nanoparticles with different sizes, Materials Letters 65 (2011) 1573–1575.

[8] F. Gao, X.Y. Chen, K.B. Yin, S.A. Dong, Z.F. Ren, F. Yuan, T. Yu, Z.G. Zou, J.M. Liu, Visible-light photocatalytic properties of weak magnetic $BiFeO_3$ nanoparticles, Advanced Materials 19 (2007) 2889–2892.

[9] S. Farhadi, N. Rashidi, Preparation and characterization of pure single-phase $BiFeO_3$ nanoparticles through thermal decomposition of the heteronuclear $Bi[Fe(CN)_6]\cdot 5H_2O$ complex, Polyhedron 29 (2010) 2959–2965.

[10] T.J. Park, G.C. Papaefthymiou, A.J. Viescas, A.R. Moodenbaugh, S.S. Wong, Size-dependent magnetic properties of single-crystalline multiferroic $BiFeO_3$ nanoparticles, Nano Letters 7 (2007) 766–772.

[11] L. Zhang, X.F. Cao, Y.L. Ma, X.T. Chen, Z.L. Xue, Polymer-directed synthesis and magnetic property of nanoparticles-assembled $BiFeO_3$ microrods, Journal of Solid State Chemistry 183 (2010) 1761–1766.

[12] S.H. Han, K.S. Kim, H.G. Kim, H.G. Lee, H.W. Kang, J.S. Kim, C.I. Cheon, Synthesis and characterization of multiferroic $BiFeO_3$ powders fabricated by hydrothermal method, Ceramics International 36 (2010) 1365–1372.

[13] J. Zou, J.Z. Jiang, Y.X. Zhang, J.A. Ma, Q.J. Wan, A comparative study of the optical, magnetic and electrocatalytic properties of nano $BiFeO_3$ with different morphologies, Materials Letters 72 (2012) 134–136.

[14] C.J. Tsai, C.Y. Yang, Y.C. Liao, Y.L. Chueh, Hydrothermally grown bismuth ferrites: controllable phases and morphologies in a mixed KOH/NaOH mineralizer, Journal of Materials Chemistry 22 (2012) 17432–17436.

[15] A. Huang, A.D. Handoko, G.K.L. Goh, P.K. Pallathadka, S. Shannigrahi, Hydrothermal synthesis of (00l) epitaxial $BiFeO_3$ films on $SrTiO_3$ substrate, CrystEngComm 12 (2010) 3806–3814.

[16] A.A. Cristóbal, P.M. Botta, Mechanochemically assisted synthesis of nanocrystalline $BiFeO_3$, Materials Chemistry and Physics 139 (2013) 931–935.

[17] X.H. Zheng, P.J. Chen, N. Ma, Z.H. Ma, D.P. Tang, Synthesis and dielectric properties of $BiFeO_3$ derived from molten salt method, Journal of Materials Science: Materials in Electronics 23 (2012) 990–994.

[18] M.M. Rashad, Effect of synthesis conditions on the preparation of $BiFeO_3$ nanopowders using two different methods, Journal of Materials Science: Materials in Electronics 23 (2012) 882–888.

[19] E. Shi, C.R. Cho, M.S. Jang, S.Y. Jeong, H.J. Kim, The formation mechanism of barium titanate thin film under hydrothermal conditions, Journal of Materials Research 9 (1994) 2914–2918.

[20] S.J. Clark, J. Robertson, Band gap and Schottky barrier heights of multiferroic $BiFeO_3$, Applied Physics Letters 90 (2007) 132903 (1–3).

[21] I. Sosnowska, T. Peterlin-Neumaier, E. Steichele, Spiral magnetic ordering in bismuth ferrite, Journal of Physics C: Solid State Physics 15 (1982) 4835–4846.